



OPEN

## Study on load reduction and vibration control strategies for semi-submersible offshore wind turbines

Dongxiao Bai<sup>1</sup>, Bing Wang<sup>2</sup>✉, Yinsheng Li<sup>1</sup> & Wancheng Wang<sup>2</sup>

Independent pitch control (IPC) is a crucial technology for enhancing the performance of wind turbines, optimizing the power output, and reducing the loads by managing each blade. This paper explores the primary vibration modes of semi-submersible wind turbines under wind-wave coupling. Given the effectiveness of pitch control in vibration suppression, this paper addresses the limitations of conventional collective pitch control (CPC) by designing an independent pitch control method based on an equivalent wind speed model (EWIPC). This model constructs an effective representation of the actual wind speed's influence on pitch angle by comprehensively considering the spatial distribution of wind speeds. This way, the control accuracy and response speed are significantly improved, making the control strategy more intuitive and efficient in complex wind speed environments. The proposed independent pitch control method is validated through simulations on the International Energy Agency (IEA) 15 MW wind turbine. The simulation results indicate that the EWIPC stabilizes wind turbine power output and reduces structural loads. Additionally, it demonstrates significant effectiveness in reducing vibrations of the blades and tower, as well as in eliminating 1P oscillations in the blade root bending moment.

**Keywords** Semi-submersible wind turbine, Independent pitch control, Equivalent wind speed model, Load reduction, Vibration suppression

With advances in wind power technology, the design and control systems of wind turbines have become increasingly complex. Early wind turbines employed simple CPC systems, where the pitch angles of all blades were adjusted simultaneously. However, as the sizes of turbines increase, the limitations of CPC have become more apparent under complex wind conditions. These issues, due to the inability to effectively balance the rotor load, result in reduced rotor efficiency, increased fatigue and damage to mechanical structures, and compromised stability and safety of the wind turbine system<sup>1,2</sup>. Compared to onshore turbines, floating wind turbines are subject to more complex vibration issues due to the interaction of wind and waves<sup>3</sup>. Therefore, investigating load and vibration issues in floating wind turbines is crucial for stabilizing power output, extending operational lifespan, and ensuring reliable performance.

Currently, the IPC is a significant research focus in wind power. It aims to optimize rotor performance, reduce load fluctuations, and enhance system stability by independently controlling the pitch angles of each wind turbine blade<sup>4–6</sup>. Significant research has been conducted on applying individual pitch control technology for load reduction in wind turbines. In Literature<sup>7</sup>, a fuzzy adaptive tuning independent pitch control (FATIPC) strategy was proposed, to optimize load control in wind turbines. The results indicate that this strategy significantly reduces the pitch bending moment at the hub, mitigates load imbalance, and reduces fatigue vibrations in key components under complex wind conditions. In Literature<sup>8</sup>, two individual pitch controllers based on disturbance adjustment control (DAC) algorithms were designed. One controller used a Turbine Symmetric-Asymmetric (TSA) model to represent wind disturbances as horizontal and shear components, While the other employed a Multi-Blade Coordinate (MBC) transformation model to describe these components as step waveform disturbances. Simulation findings show that these proposed control strategies effectively reduce blade imbalance loads. In Literature<sup>9</sup>, a model predictive controller was enhanced with a linear processing module for real-time pitch signal correction in the IPC. The results demonstrate that this strategy significantly reduces blade root load fluctuations. In Literature<sup>10</sup>, a two-degree-of-freedom robust individual pitch control (2DoF RIPC)

<sup>1</sup>College of Electrical and Power Engineering, Hohai University, Nanjing, China. <sup>2</sup>College of Artificial Intelligence and Automation, Hohai University, Nanjing, China. ✉email: icekingking@hhu.edu.cn

Parameter	IEA 15 MW
Rated power	15 MW
N blades	3
Rotor diameter	240 m
Hub height	150 m
Rotor orientation	Upwind
Cut-in wind speed	3 m/s
Rated wind speed	10.74 m/s
Cut-out wind speed	25 m/s
Design tip speed ratio	9
Drive train	Low speed. Direct drive

**Table 1.** Basic parameters of wind turbines.

Working conditions	Wave height(m)	Period(s)	Wind speed(m/s)	Control
E01 (Steady Wind)	1.1	8.5	8	Variable speed
E02 (Steady Wind)	1.1	8.5	10.74	Variable speed, Pitch
E03 (Steady Wind)	1.1	8.5	13	Pitch
E04 (Turbulent wind)	1.1	8.5	10.74	Variable speed, Pitch
E05 (Steady Wind)	10	20	13	Pitch

**Table 2.** Parameters of design conditions.

strategy was presented, addressing the complexity of parameter tuning using a reference model approach for setting closed-loop system responses. The results show that this controller effectively reduces loads on the rotor and tower without affecting power. In Literature<sup>11</sup>, a detailed comparison of various IPC strategies, including Model Predictive Control (MPC),  $H_{\infty}$ , and PI control, was provided. The results using the National Renewable Energy Laboratory (NREL) 5 MW nonlinear wind turbine show that the  $H_{\infty}$  based IPC performs better in reducing blade root bending moments and damage equivalent loads under varying wind speeds and turbulence intensities.

While these studies effectively validate the load reduction capabilities of IPC strategies, they not only lack research on wind turbine vibrations but also fail to provide an in-depth description of the aerodynamic effects of real wind speeds on pitch control during turbine operation.

This paper investigates the main vibration modes of the semi-submersible IEA 15 MW wind turbine<sup>12,13</sup> using OpenFAST under combined wind and wave conditions. An accurate equivalent wind speed model is developed, considering the effects of the floating platform's motion, wind shear, and tower shadow. The model combines azimuth feedforward control and blade unbalance load feedback to design the EWIPC. The effectiveness of the proposed control strategy is evaluated through simulations comparing it with this NREL's reference open-source independent pitch control (ROSIPC)<sup>14</sup>. The results show that the controller effectively reduces fatigue loads and dampens vibration for semi-submersible wind turbines.

### Analysis of major vibration modes in semi-submersible wind turbines

A fully coupled time-domain simulation of the semi-submersible IEA 15 MW wind turbine system is conducted using OpenFAST to investigate the major vibration modes under combined wind and wave conditions<sup>15,16</sup>. In this case, the basic parameters of the wind turbine are shown in Table 1. The sea states are categorized into two conditions: normal operating conditions with a wave height of 1.1 m and a period of 8.5 s, and extreme survival conditions with a wave height of 10 m and a period of 20 s. The wind conditions are also divided into two types: steady wind and turbulent wind. For turbulent wind, the settings include: (i) the Kaimal model; (ii) IEC standard IE-3; (iii) turbulence intensity B; (iv) the power-law wind profile.

Given that the wind turbine's rated wind speed is 10.74 m/s, the design conditions based on its parameters, sea state, and wind conditions are summarized in Table 2.

### Analysis of major vibration modes of the blades

The vibration modes on the blades of the semi-submersible wind turbine include flapwise, edgewise, and torsional displacements at the blade tip. Simulations are conducted under all conditions to investigate the main vibration modes. The simulation results show that torsional displacement is zero, while flapwise and edgewise displacements vary as illustrated in Fig. 1.

As shown in Fig. 1, based on the amplitude magnitude, the primary vibration mode of the blades is flapwise displacement.

Based on Fig. 1(a): (i) E02 vs. E01 and E05 vs. E03: Wind loads have a greater effect on flapwise displacement compared to wave loads. (ii) E04 vs. E02: Turbulent wind has a more pronounced effect on flapwise displacement. (iii) E03 vs. E02: Pitch control effectively reduces variations in flapwise displacement.

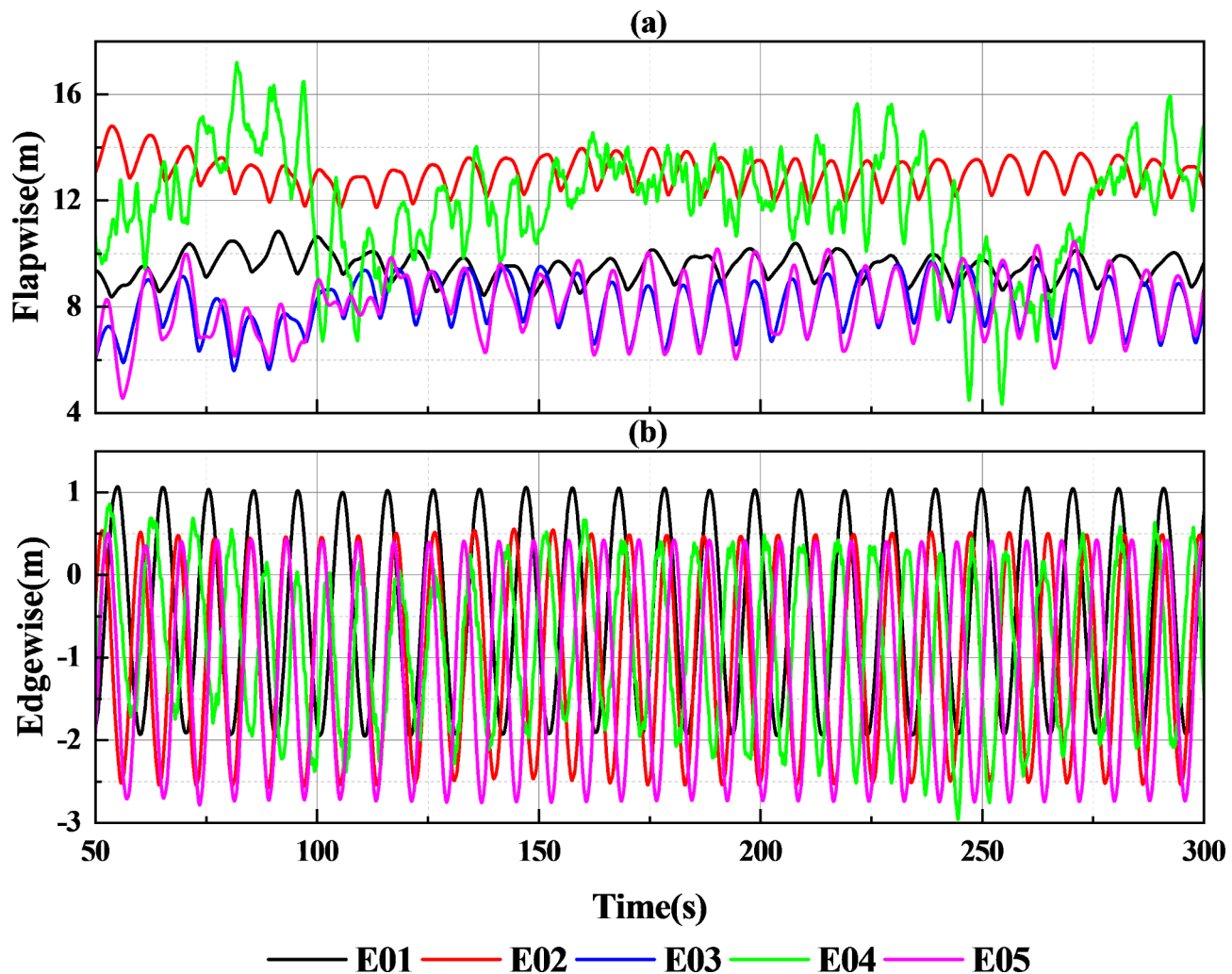


**Fig. 1.** Time domain analysis of blade tip displacements.

#### Analysis of major vibration modes of the tower

The vibration modes of the tower in a semi-submersible wind turbine include fore-aft, side-to-side, and axial deflections at the tower top. Simulations are conducted under all conditions to investigate the main vibration modes. The simulation results show that axial deflection is zero, while fore-aft and side-to-side deflections vary as illustrated in Fig. 2.

As shown in Fig. 2, based on the amplitude magnitude, the primary vibration mode of the tower is the fore-aft deflection of the tower top.

Based on Fig. 2(a): (i) E02 vs. E01 and E05 vs. E03: Wind loads have a significant impact on fore-aft deflections compared to wave loads. (ii) E04 vs. E02: Turbulent wind notably affects the fore-aft deflections of the tower top. (iii) E03 vs. E02: Pitch control effectively mitigates variations in the fore-aft deflection of the tower top.

#### Analysis of major vibration modes of the platform

The vibration modes of the platform include surge, sway, heave, roll, pitch, and yaw. Simulations are conducted under all conditions to investigate the main vibration modes. The simulation results for surge, sway, and heave are shown in Fig. 3, while those for roll, pitch, and yaw are shown in Fig. 4.

From Fig. 3, based on the amplitude magnitude, the primary vibration mode of the platform translations is surge.

Based on Fig. 3(a): (i) E02 vs. E01 and E05 vs. E03: Wind loads have a more pronounced effect on surge compared to wave loads. (ii) E04 vs. E02: Both turbulent winds and irregular waves have a small effect on surge, but turbulent winds are more pronounced. (iii) E03 vs. E02: Pitch angle control effectively mitigates variations in surge.

From Fig. 4, based on the amplitude magnitude, the primary vibration mode of the platform is pitch.

Based on Fig. 4(a): (i) E02 vs. E01 and E05 vs. E03: Wind loads have a significant impact on pitch compared to wave loads. (ii) E04 vs. E02: Turbulent wind has a substantial impact on pitch. (iii) E03 vs. E02: Pitch angle control effectively reduces variations in pitch.

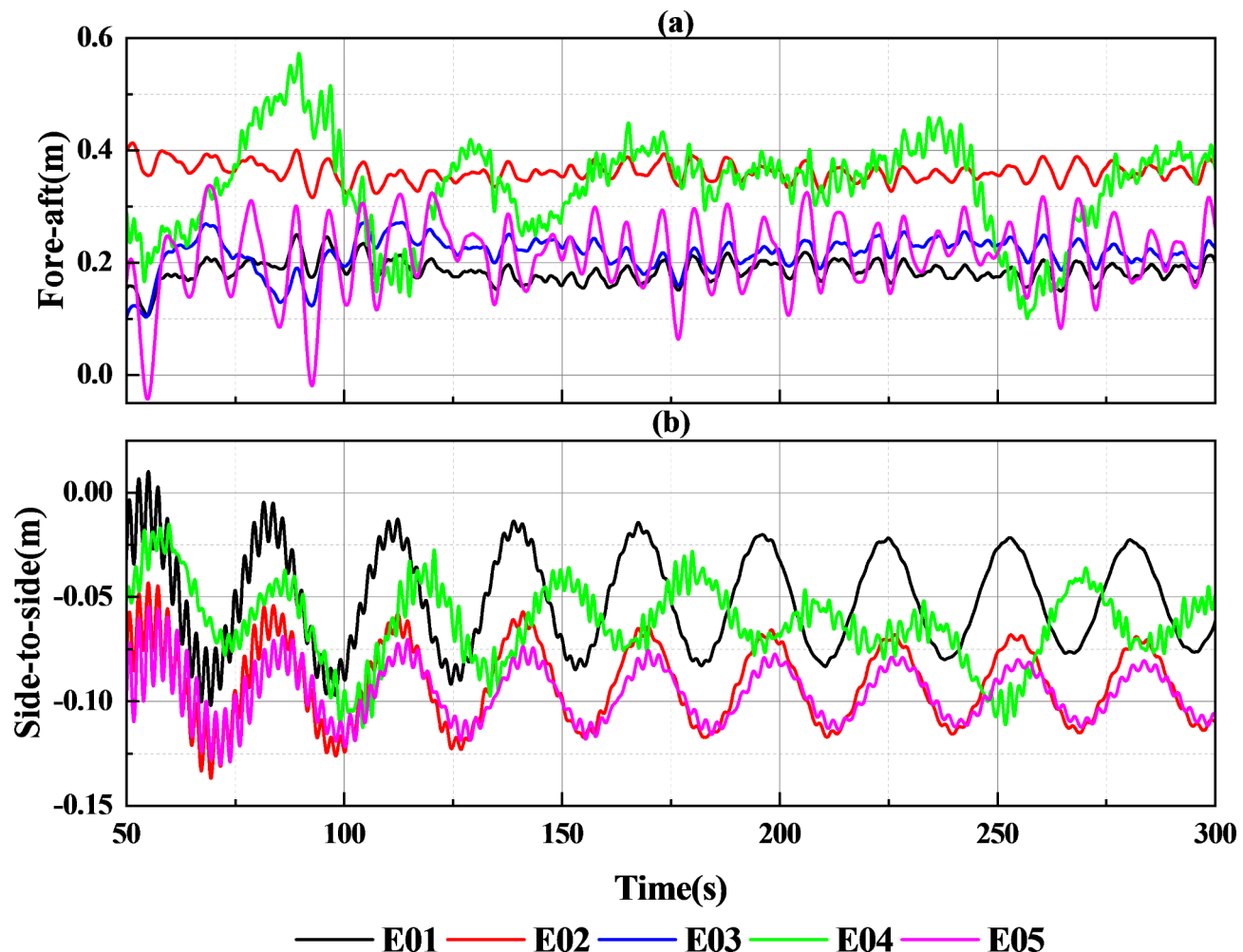


**Fig. 2.** Time domain analysis of tower top displacements.

In summary, the primary vibration modes of the semi-submersible wind turbine components include flapwise displacement, tower top fore-aft deflection, and surge and pitch. The effects of wind-wave loads on these vibration modes vary, and pitch control effectively suppresses the vibrations.

#### Equivalent wind speed model

Natural wind varies over time and space, causing changes in wind speed and unevenness within the wind turbine plane, which results in imbalanced aerodynamic loads on the blades. Key factors influencing the imbalance of aerodynamic loads on wind turbine blades include the motion of the supporting structure, wind shear effects, and tower shadow effects.

#### Influence of basic platform movement

Due to the concentration of the center of gravity of the floating wind turbine system on the platform, movements of the center of gravity, particularly in pitch, can cause significant motion of the wind turbine. Therefore, it is necessary to establish a relative wind speed model that accounts for the effects of base platform motion.

The displacement of the hub affected by the platform motion,  $x_{hub}$  is given by<sup>17</sup>:

$$x_{hub} = x_{surge} + \sin(\theta_{pitch})H_{hub} \quad (1)$$

where  $x_{surge}$  is the surge displacement of the platform,  $\theta_{pitch}$  is the pitch angle of the platform, and  $H_{hub}$  is the hub height.

The relative effective wind speed at the hub,  $V_{hub}$  is given by:

$$V_{hub} = V_{wind} - x_{hub} + \cos(\Psi) \frac{3}{2H_{hub}} rx_{hub} \quad (2)$$

where  $V_{wind}$  is the incoming wind speed,  $\Psi$  is the blade azimuth angle, and  $r$  is the radial distance from the hub to the blade element.

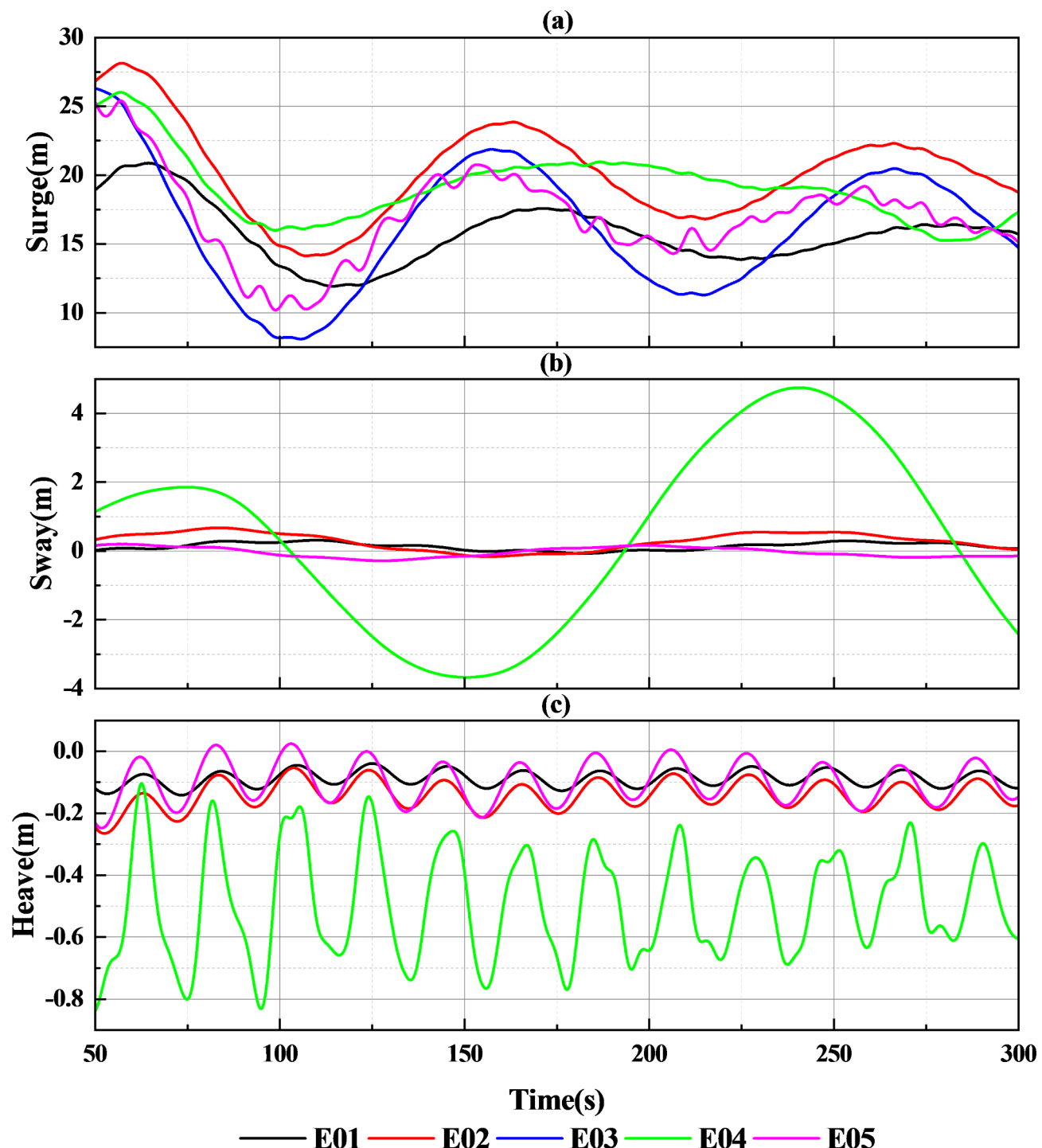


**Fig. 3.** Time domain analysis of platform translations.

#### Wind shear<sup>18</sup>

Wind shear effects refer to the wind speed gradients generated by variations in wind speed with height. These effects affect the aerodynamic loads, power output, and stability of wind turbines, and can be described using an exponential model as follows:

$$\frac{V}{V_{hub}} = \left( \frac{H}{H_{hub}} \right)^n \quad (3)$$

where  $H$  is the vertical height above the ground,  $V$  is the wind speed at height  $H$ , and  $n$  is the wind shear coefficient.

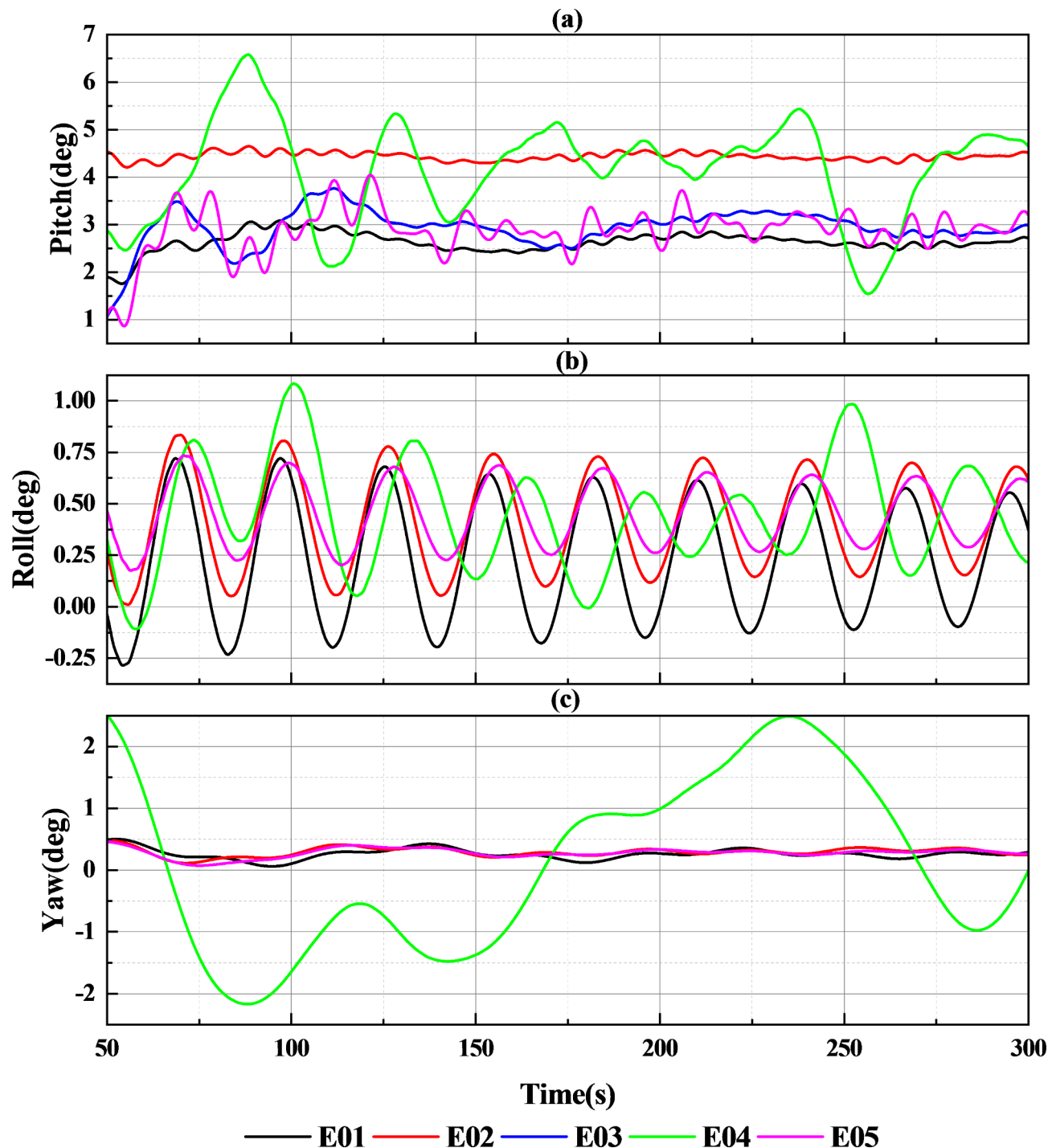


Fig. 4. Time domain analysis of platform rotamentals.

#### Tower shadow<sup>19</sup>

The tower shadow refers to the impact of the wind turbine tower on the wind speed and airflow distribution around the rotor blades. Since the wind turbine studied is an upwind turbine, the tower shadow effect it experiences is described by:

$$v(x, y) = V_0 R_{tow}^2 \frac{y^2 - x^2}{(y^2 + x^2)^2} \quad (4)$$

where  $V_0$  is the spatially averaged wind speed,  $R_{tow}$  is the tower radius,  $y$  is the distance in the  $y$ -direction from the blade element to the tower axis,  $x$  is the distance in the  $x$ -direction from the blade element to the tower axis, and  $v(x, y)$  represents the variation in wind speed due to the tower shadow effect.

### Wind speed model

Based on the blade azimuth angle and the radial distance from the element to the rotor center, the rotor sweep plane is divided into four regions, as shown in Fig. 5, to describe the wind speed.

Region ① represents the upper half of the rotor sweep plane and is influenced only by wind shear effects. Regions ②, ③, and ④ are in the lower half of the rotor sweep plane. Region ③ is also influenced only by wind shear effects but requires a separate description due to different boundary conditions compared to Region ①. Regions ② and ④ are affected by both wind shear and tower shadow effects, and the wind speed in these regions is described separately due to differing boundary conditions.

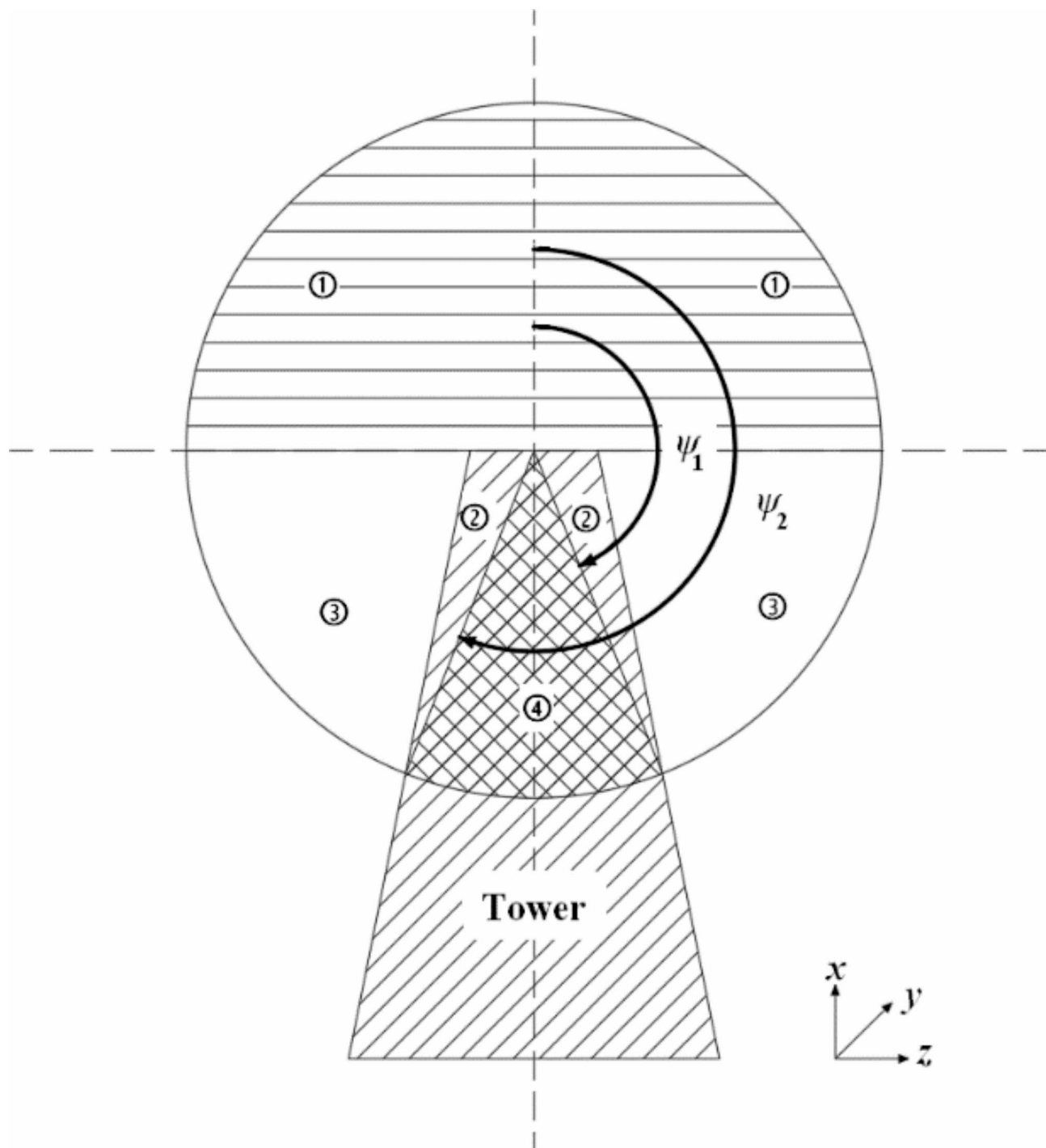


**Fig. 5.** Wind speed zone division on the rotor surface.

## Individual pitch control

From Fig. 6, the control process is divided into two parts: (i) Azimuth angle feedforward-based individual pitch control effectively manages periodic load imbalances such as those caused by wind shear and tower shadow effects. (ii) The blade root unbalance load feedback controller effectively addresses random aerodynamic load imbalances at the blade root, thereby enhancing aerodynamic load reduction.

### Azimuth feedforward control

During turbine operation, the equivalent wind speed at different rotor plane positions varies with each blade's azimuth angle. The equivalent wind speed for each blade can be determined using azimuth-dependent weighting factors<sup>20</sup>. For a three-blade turbine, the pitch angle weighting factors for the three blades are as follows:

$$K_b = \frac{3V_b^l}{\sum_{b=1}^3 V_b^l} \quad b = 1, 2, 3 \quad (5)$$

Where  $V_b$  represents the equivalent wind speed for blade  $b$ , typically measured at 3/4 of the blade radius  $R$ ;  $l$  is the exponent coefficient related to the wind speed model.

### Blade root unbalanced load feedback

The blade root unbalance loads,  $M_1$ ,  $M_2$ , and  $M_3$ , are converted to  $M_{tilt}$  and  $M_{yaw}$  in the hub coordinate system, and the required Coleman transform formula<sup>5,11,21</sup> is:

$$\begin{bmatrix} M_{tilt} \\ M_{yaw} \end{bmatrix} = \frac{2}{3} \begin{bmatrix} \sin \Psi \sin \left( \Psi + \frac{2}{3}\pi \right) \sin \left( \Psi + \frac{4}{3}\pi \right) \\ \cos \Psi \cos \left( \Psi + \frac{2}{3}\pi \right) \cos \left( \Psi + \frac{4}{3}\pi \right) \end{bmatrix} \begin{bmatrix} M_1 \\ M_2 \\ M_3 \end{bmatrix} \quad (6)$$

Converting  $\beta_d$  and  $\beta_q$  in the hub coordinate system, to the corrected values of pitch angle  $\Delta\beta_1$ ,  $\Delta\beta_2$ , and  $\Delta\beta_3$  for each blade, the required Coleman inverse transform formula<sup>5,11,21</sup> is:

$$\begin{bmatrix} \Delta\beta_1 \\ \Delta\beta_2 \\ \Delta\beta_3 \end{bmatrix} = \begin{bmatrix} \sin \Psi & \cos \Psi \\ \sin \left( \Psi + \frac{2}{3}\pi \right) \cos \left( \Psi + \frac{2}{3}\pi \right) \\ \sin \left( \Psi + \frac{4}{3}\pi \right) \cos \left( \Psi + \frac{4}{3}\pi \right) \end{bmatrix} \begin{bmatrix} \beta_d \\ \beta_q \end{bmatrix} \quad (7)$$

## Simulation results analysis

Due to the minor influence of wave loads, steady and turbulent winds of 18 m/s are selected for the simulation. The simulation lasted for 1000 s with a step size of 0.0125 s, and results from 300 to 600 s are analyzed.

### Steady wind field

Figure 7 shows that the pitch angle weighting coefficients in EWIPC vary in a quasi-sinusoidal cycle between 0.7 and 1.25. In the EWIPC control system, the pitch angle weighting coefficients vary in a quasi-sinusoidal manner between 0.7 and 1.25. Since these coefficients are related to the azimuth angle, the phase differences between  $K_1$ ,  $K_2$ , and  $K_3$  are  $\pm 120^\circ$ .

From Fig. 8; Table 3, it can be observed that under IPC control, the blade pitch angles of the three blades exhibit gain and phase shift variations based on the CPC. The amplitudes and fluctuations of the pitch angles for the three blades under the same control scheme are largely consistent. Both the amplitude and fluctuation of the pitch angles are reduced under EWIPC relative to ROSIPC.

As shown in Fig. 9, the results of the IPC methods are largely consistent, both achieving load reduction while maintaining stable power. Compared to ROSIPC, the fluctuations in the blade root unbalanced loads under EWIPC are significantly reduced. This indicates that EWIPC is more effective in mitigating unbalanced loads on the blades, resulting in a more efficient load reduction effect.

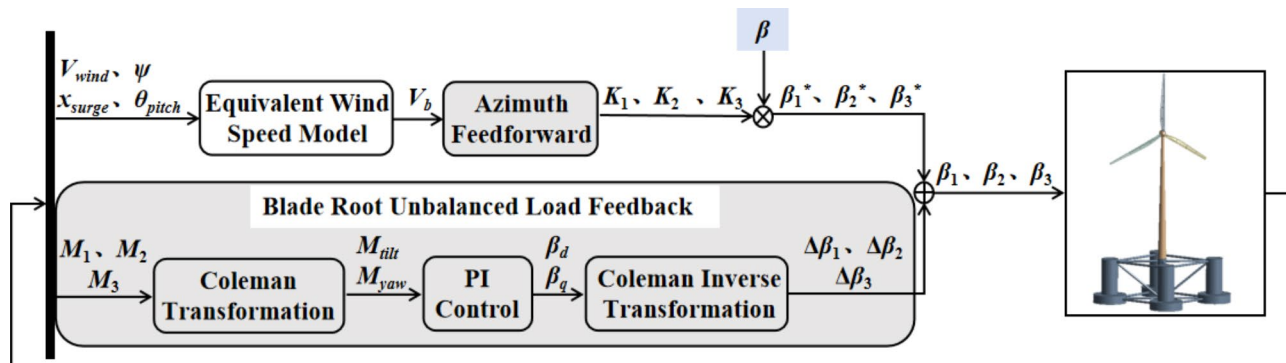


**Fig. 6.** Individual pitch control system control block diagram.

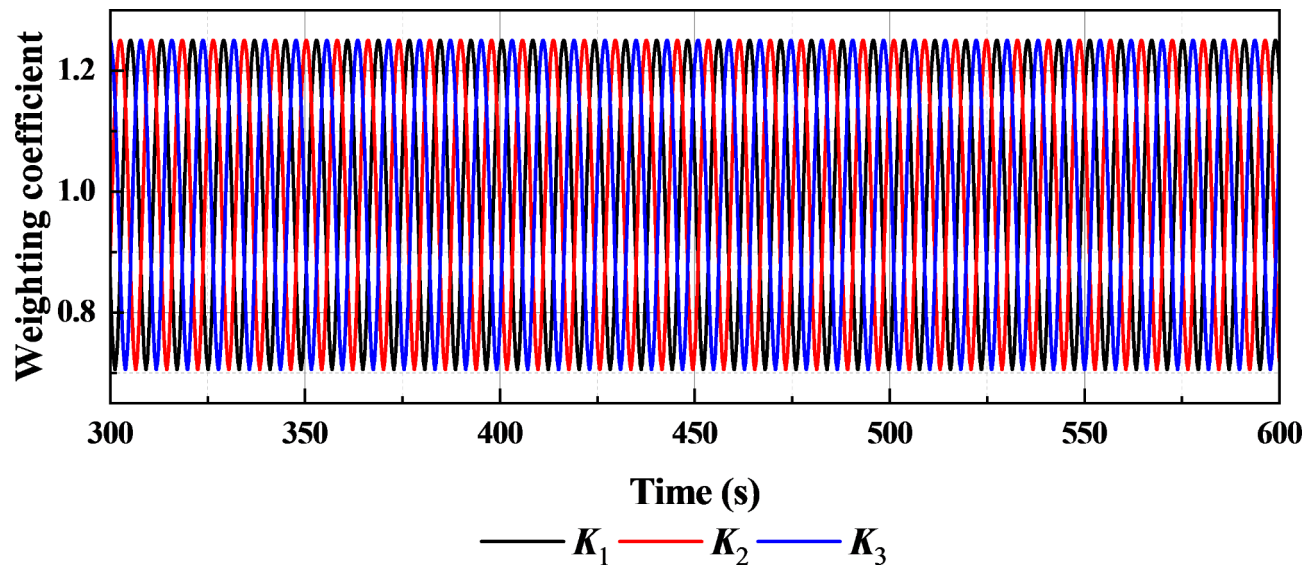


Fig. 7. Weighting coefficient by EWIPC.

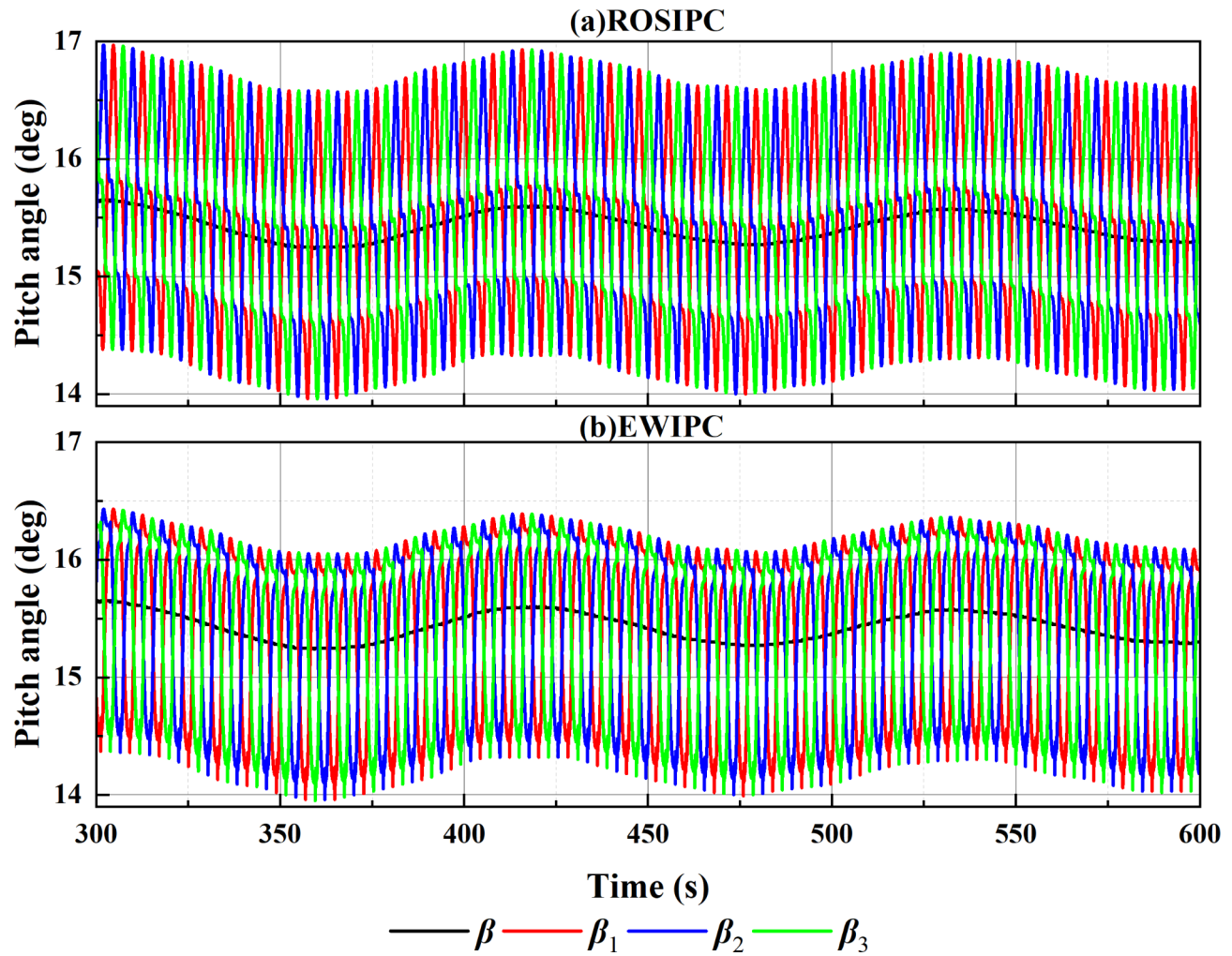
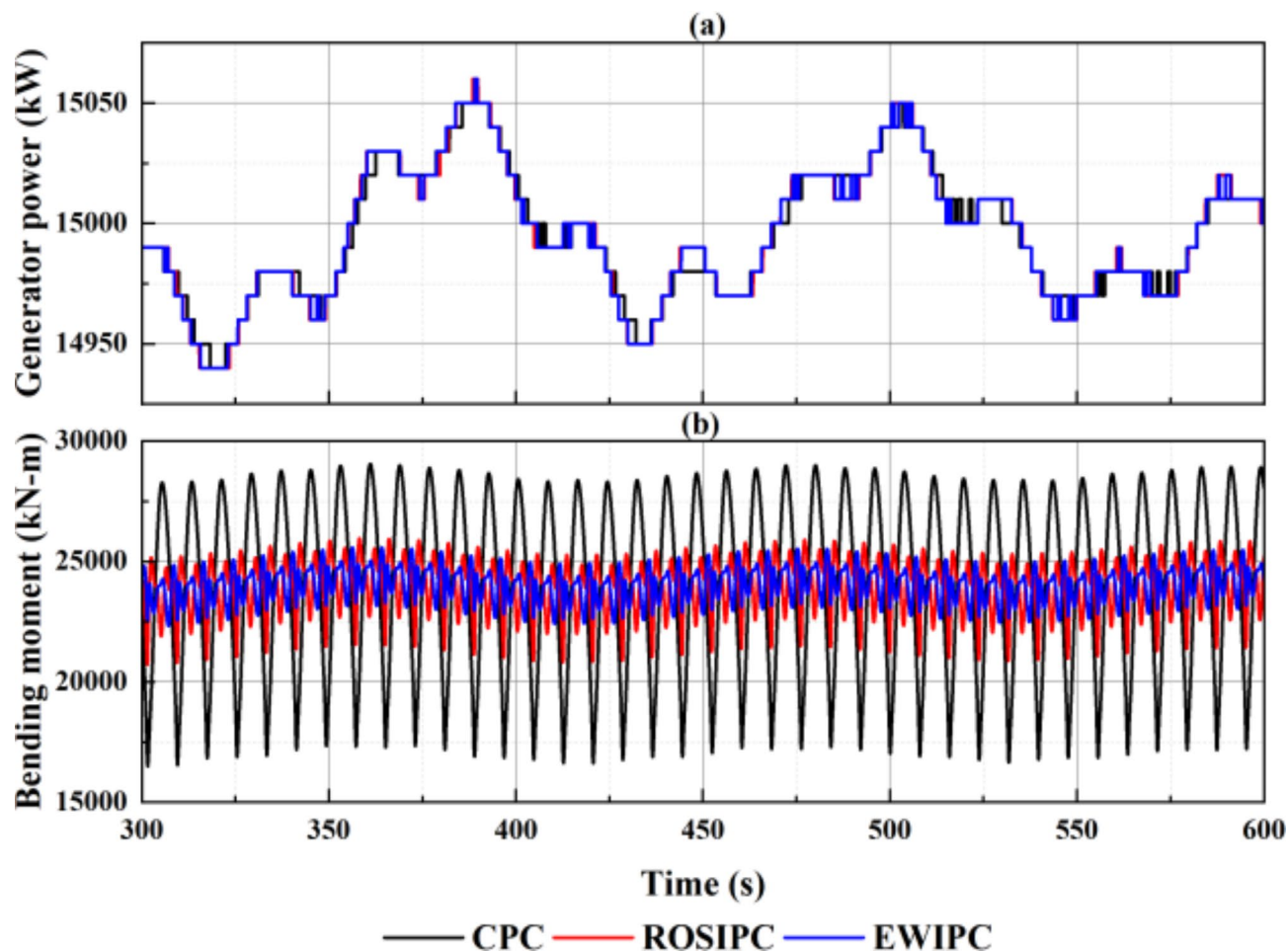


Fig. 8. Pitch angle by ROSIPC and EWIPC.

Control method	Parameters	Maximum	Minimum	Mean	Std. deviation
ROSIPC	$\beta_1$	16.9700	13.9600	15.4317	0.7409
	$\beta_2$	16.9700	13.9600	15.4363	0.7403
	$\beta_3$	16.9600	13.9600	15.4254	0.7383
EWIPC	$\beta_1$	16.4300	13.9600	15.4282	0.7182
	$\beta_2$	16.4300	13.9600	15.4326	0.7190
	$\beta_3$	16.4200	13.9500	15.4247	0.7189

**Table 3.** Time-domain statistics of pitch angle.**Fig. 9.** Time domain analysis of important parameters.

From Fig. 10, it can be seen that in the principal mode directions of the wind turbine components, both IPC methods demonstrate significant vibration suppression effects, except for platform surge. Compared to ROSIPC, EWIPC shows a notable decrease in amplitude in the blade flapping displacement and the tower top fore-aft deflection. However, the results for platform surge and pitch are largely consistent between the two control schemes.

The blade root bending moment exhibits periodic variation and can be decomposed into a DC component, a fundamental frequency component (i.e., 1P component), and higher-order harmonic components<sup>22,23</sup>. The 1P component is the primary contributor to the oscillatory bending moment, and research on IPC aims to suppress the loads associated with the 1P component.

From Fig. 11, it is evident that both IPC controllers effectively attenuate the 1P frequency (approximately 0.125 Hz), significantly reducing its amplitude. However, the ROSIPC controller exhibits increased amplitude at the 2P and 4P frequencies.

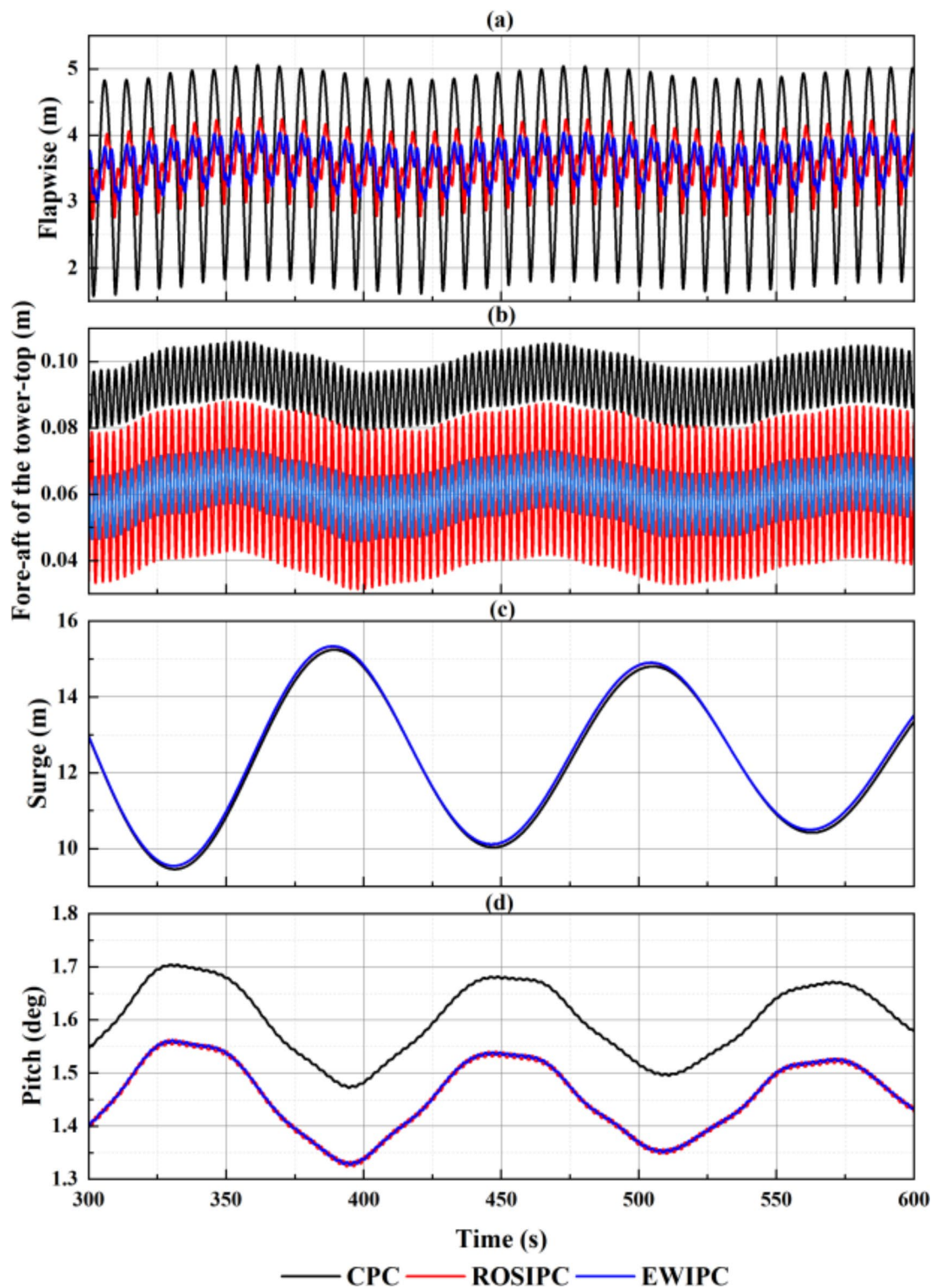


**Fig. 10.** Time domain analysis of major vibration modes.

#### Turbulent wind field

As illustrated in Fig. 12, the variation of pitch angle weighting coefficients under EWIPC is largely consistent with the results obtained under a steady wind field. This may be due to the compensatory effect of the foundation platform's motion, which addresses the uneven wind speed issues associated with turbulent wind.

From Fig. 13; Table 4, it can be seen that the effects of different control strategies on the pitch angles are generally similar to those under a steady wind field. However, the fluctuations in turbulent wind speed result

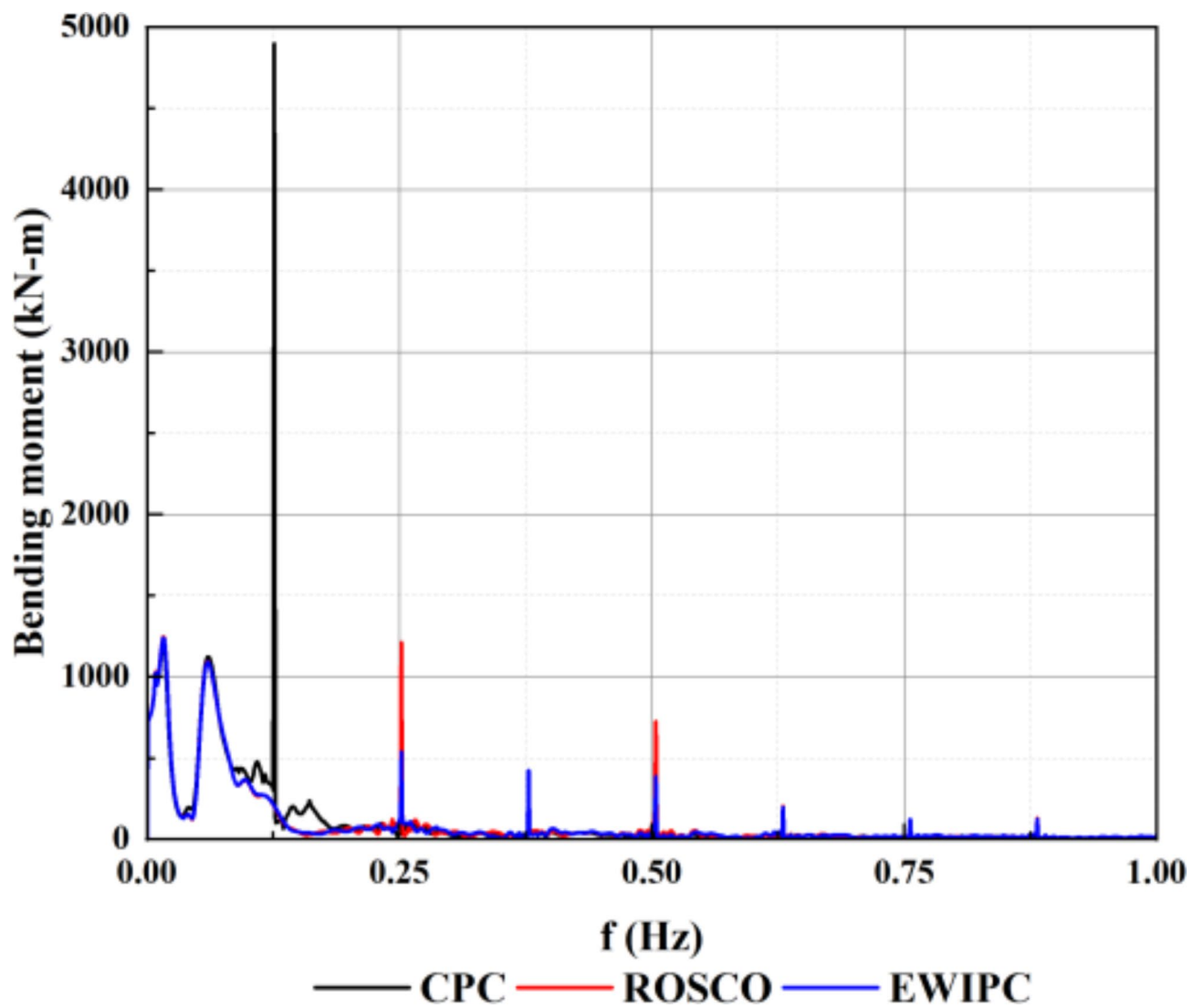


Fig. 11. Frequency domain analysis of blade root bending moment.

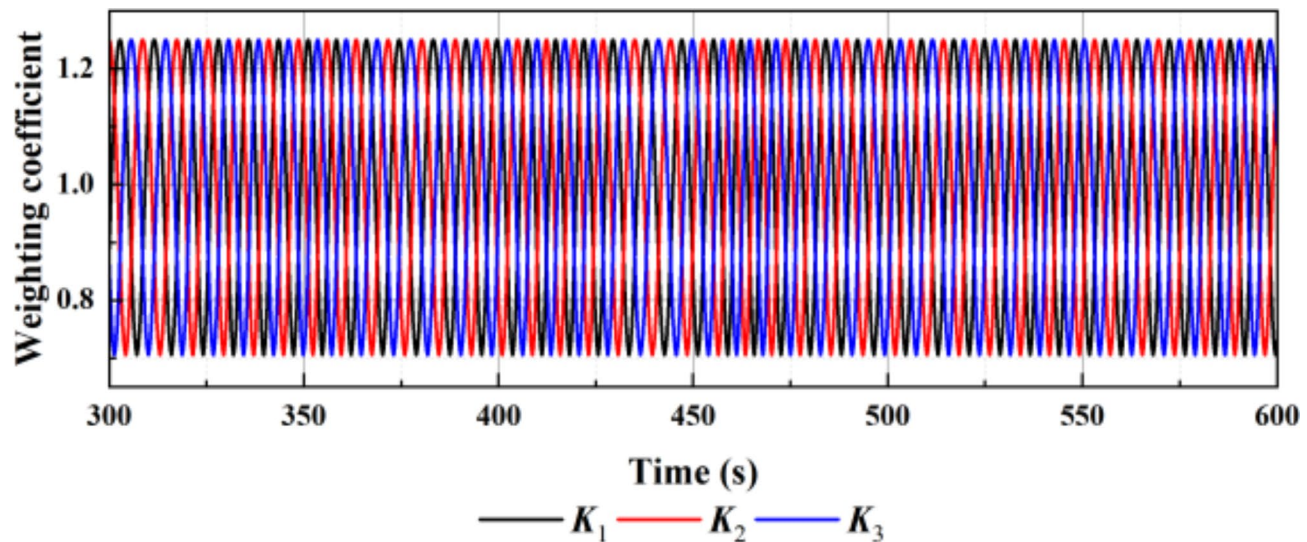
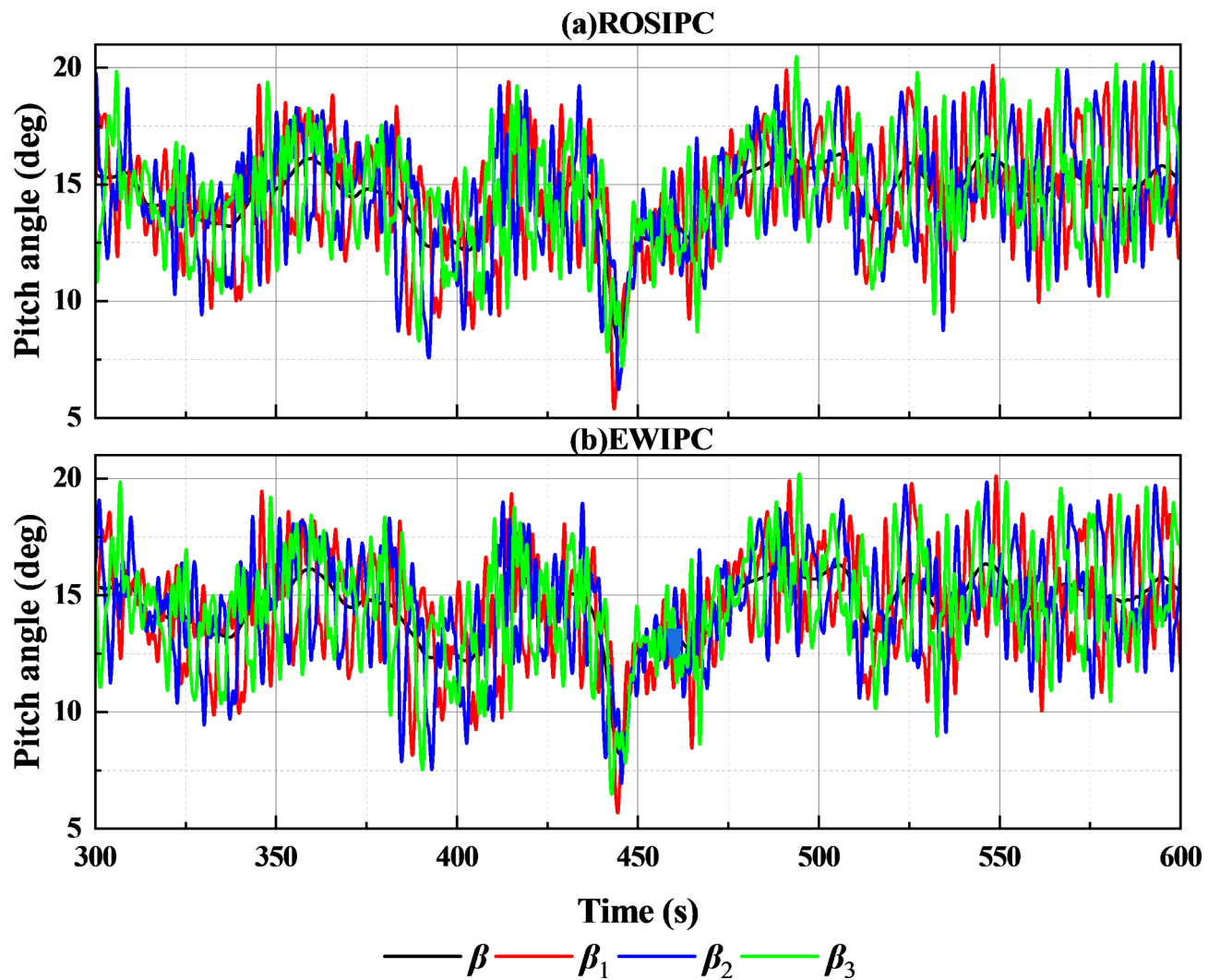


Fig. 12. Weighting coefficient by EWIPC.



**Fig. 13.** Pitch angle by ROSIPC and EWIPC.

Control method	Parameters	Maximum	Minimum	Mean	Std. deviation
ROSIPC	$\beta_1$	20.1100	5.3820	14.4522	2.3092
	$\beta_2$	20.2500	6.2130	14.4675	2.3211
	$\beta_3$	20.4800	7.1970	14.4879	2.2740
EWIPC	$\beta_1$	20.1200	5.6800	14.4521	2.2570
	$\beta_2$	19.8500	6.9440	14.4353	2.2990
	$\beta_3$	20.2000	6.4810	14.4578	2.2817

**Table 4.** Time-domain statistics of pitch angle.

in an increase in the amplitude of the pitch angles, and the advantages of EWIPC are less pronounced under a turbulent wind field.

As shown in Figs. 14 and 15, although both IPC strategies continue to achieve load reduction and vibration suppression, their effectiveness is less pronounced compared to results under a steady wind field. The vibration amplitude in the tower fore-aft direction and platform heave increases. However, EWIPC performs slightly better than ROSIPC in these aspects.

From Fig. 16, both IPC strategies effectively regulate the 1P component, but the values of higher harmonic components are slightly higher than those under CPC. Compared to ROSIPC, the fluctuations in EWIPC are slightly smaller.

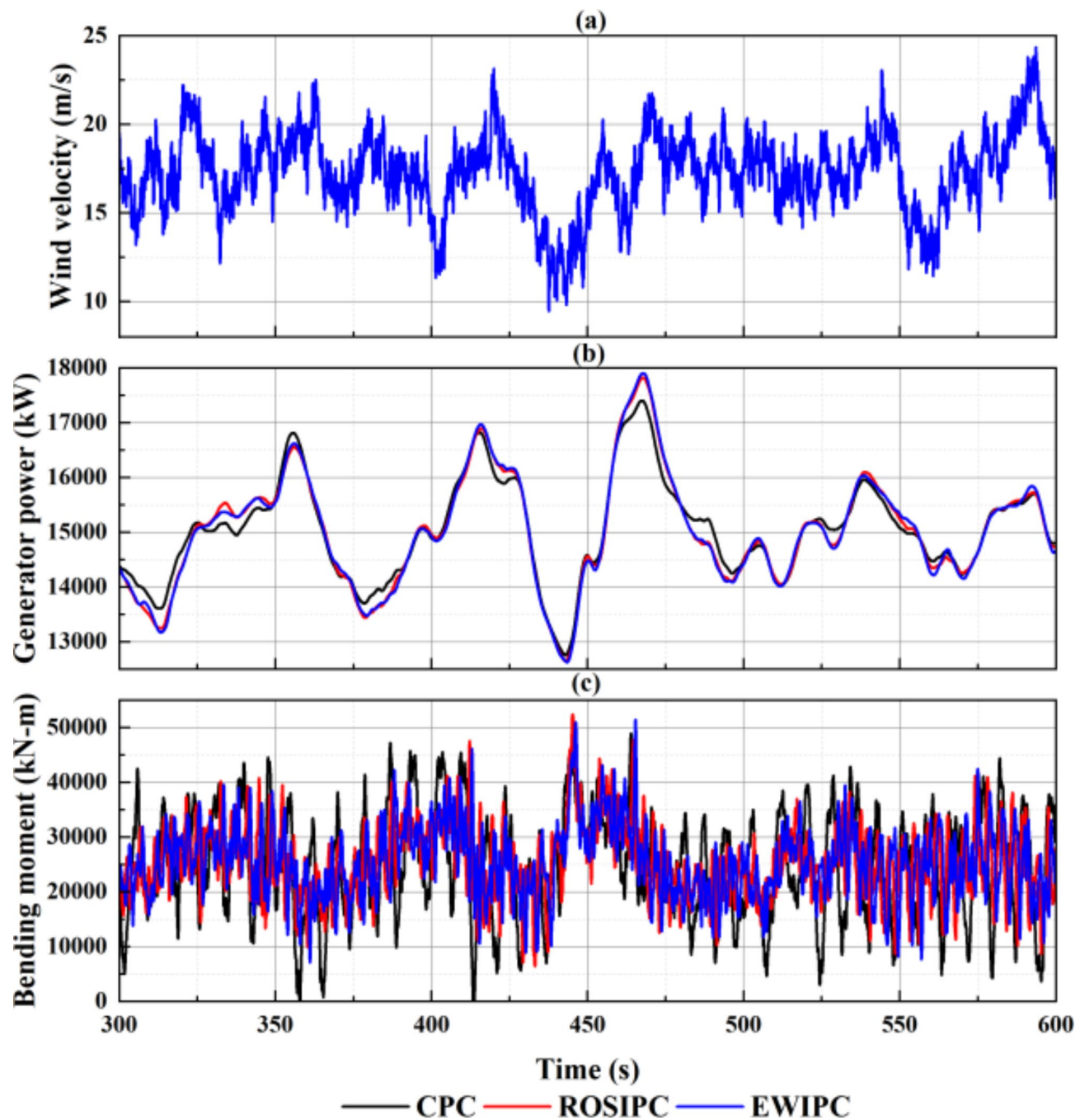


**Fig. 14.** Time domain analysis of important parameters.

### Conclusion

This paper proposes an independent pitch control based on an equivalent wind speed model. Considering the effects of basic platform motion, wind shear, and tower shadow on the actual wind speed, the control strategy incorporates azimuthal angle feedforward control and blade unbalance load feedback. Simulations using the IEA 15 MW turbine demonstrate the effectiveness of the proposed control. The main findings as follows:

- The primary vibration modes of the semi-submersible wind turbine components include blade flapwise displacement, tower top fore-aft deflection, surge, and pitch.
- Pitch control effectively suppresses vibrations.
- IPC control is effective in both load reduction and vibration suppression. Overall, the designed EWIPC demonstrates superior performance.
- The EWIPC controller effectively regulates the 1P frequency component of the blade root bending moment.

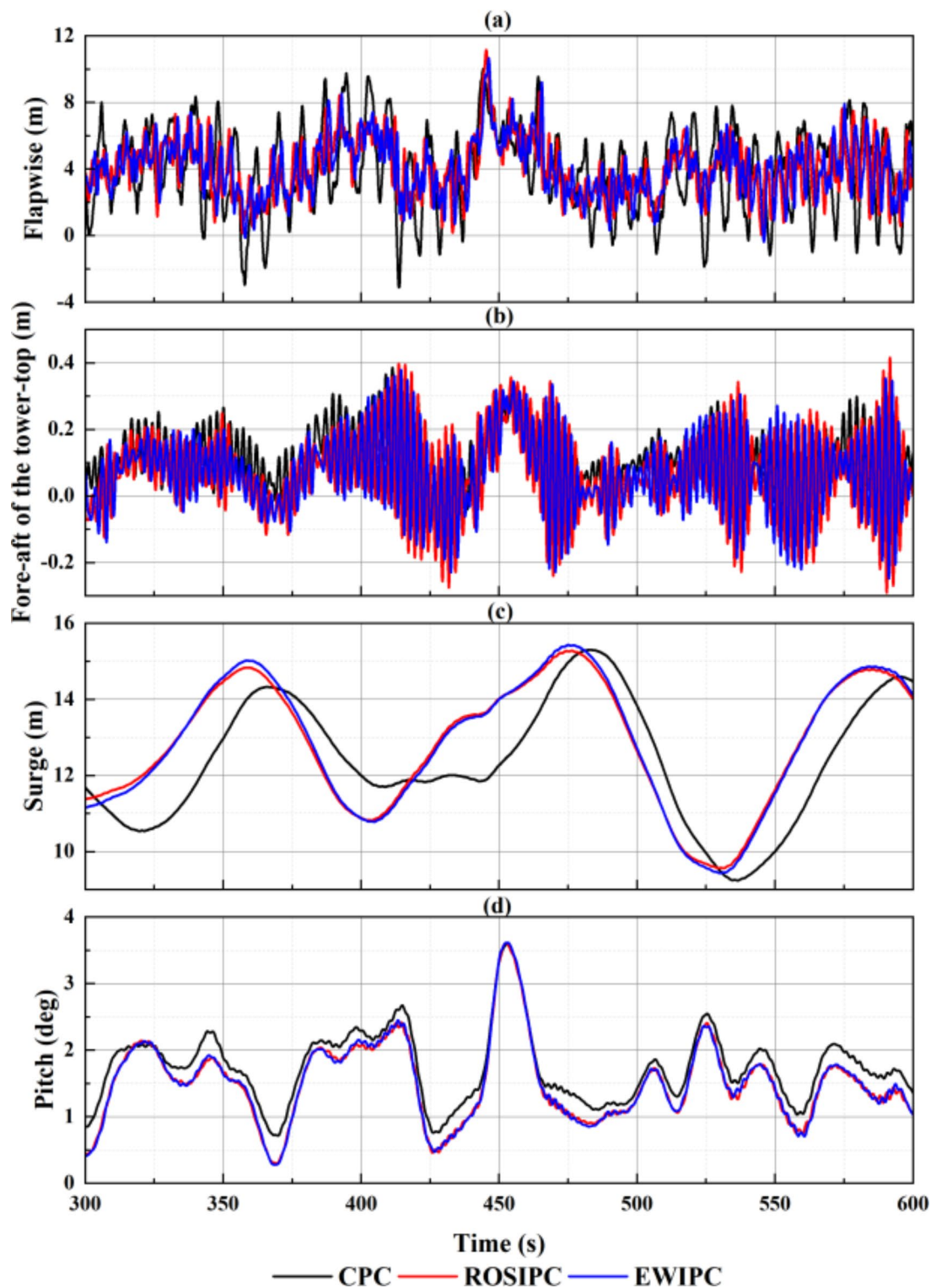


**Fig. 15.** Time domain analysis of major vibration modes.

These research findings aim to ensure the stable operation and extend the lifespan of wind turbines, and to provide a reference for load reduction and vibration suppression control in offshore floating wind turbines.

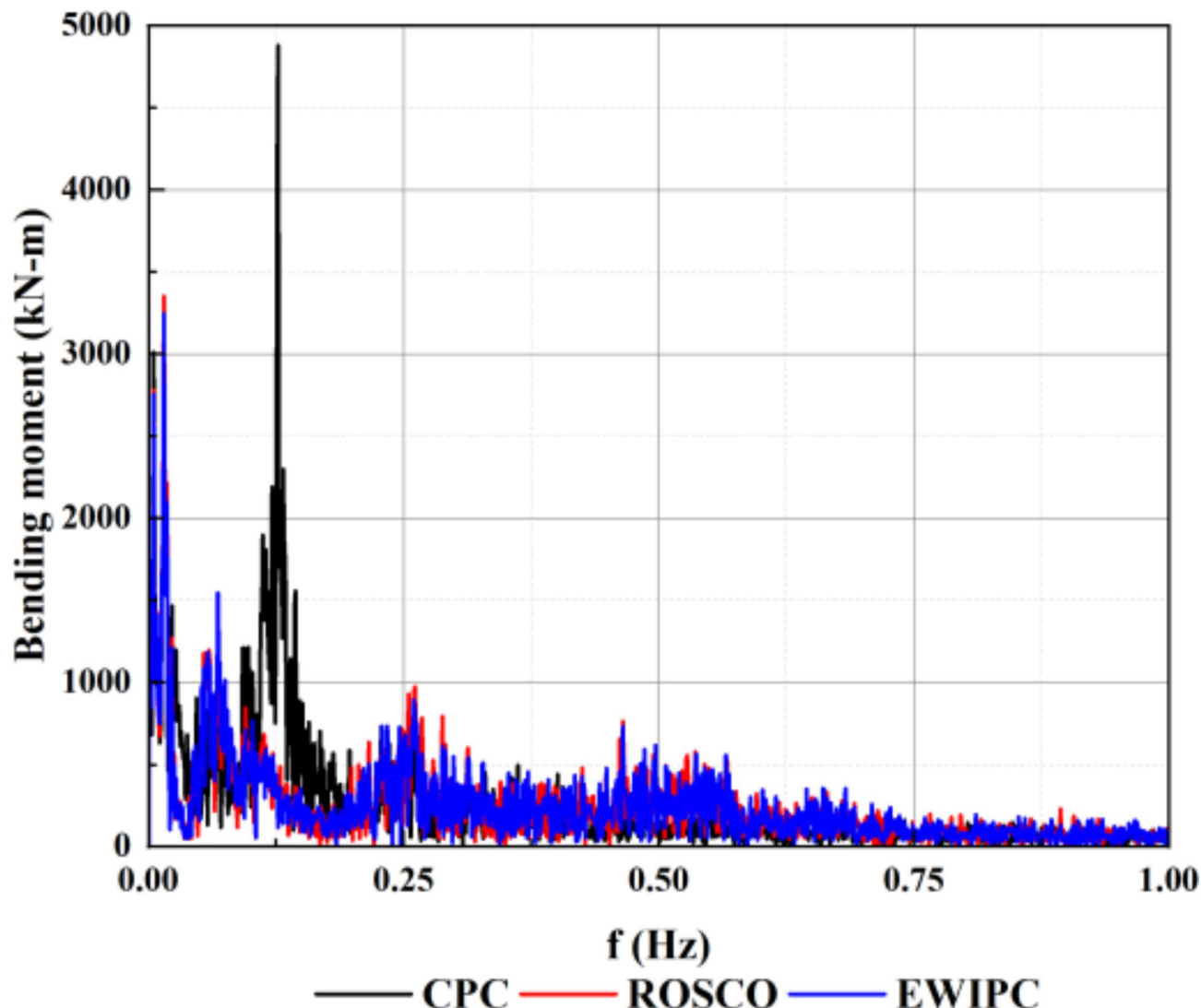


**Fig. 16.** Frequency domain analysis of blade root bending moment.

#### Data availability

The datasets used and/or analysed during the current study available from the corresponding author on reasonable request.

Received: 20 August 2024; Accepted: 3 January 2025

Published online: 07 January 2025

#### References

1. Fitzgerald, B. & Sarkar, S. Observer based pitch control for load mitigation and power regulation of floating offshore wind turbines. *Journal of Physics: Conference Series*, 2647. (2024). <https://doi.org/10.1088/1742-6596/2647/3/032003>
2. Sun, H., Yan, L. & Zhang, N. Research on Control Technology of Pitch for large wind turbine. *DEStech Trans. Environ. Energy Earth Sci.* <https://doi.org/10.12783/DTEEES/EPEE2017/18115> (2018).
3. Roh, C., Ha, Y. J., Ahn, H. J. & Kim, K. A comparative analysis of the characteristics of platform motion of a floating Offshore wind turbine based on Pitch controllers. *Energies* <https://doi.org/10.3390/en15030716> (2022).
4. Le Fouest, S. & Mullenens, K. Optimal blade pitch control for enhanced vertical-axis wind turbine performance. *Nat. Commun.* 15. <https://doi.org/10.1038/s41467-024-46988-0> (2024).
5. Lara, M., Mulders, S. P., van Wingerden, J., Vázquez, F. & Garrido, J. Analysis of Adaptive Individual Pitch Control Schemes for Blade Fatigue Load Reduction on a 15 MW wind turbine. *Appl. Sci.* <https://doi.org/10.3390/app14010183> (2023).
6. Sarkar, S., Fitzgerald, B. & Basu, B. Individual Blade Pitch Control of Floating Offshore Wind Turbines for load mitigation and power regulation. *IEEE Trans. Control Syst. Technol.* 29, 305–315. <https://doi.org/10.1109/TCST.2020.2975148> (2020).
7. Li, S. et al. Independent Pitch Controller based on Fuzzy Adaptive Tuning PI for Load Mitigation of Large Land Wind Turbine. *Journal of Physics: Conference Series*, 2655. (2023). <https://doi.org/10.1088/1742-6596/2655/1/012007>
8. Wang, N., Wright, A. D. & Johnson, K. E. Independent blade pitch controller design for a three-bladed turbine using disturbance accommodating control. 2016 American Control Conference (ACC), 2301–2306. (2016). <https://doi.org/10.1109/ACC.2016.7525261>

9. Lin, Q., Liu, Z. & Real-Time Modified Predictive Control Model for Large Scale Wind Turbine Pitch System. 2024 IEEE 13th Data Driven Control and Learning Systems Conference (DDCLS), 541–545. (2024). <https://doi.org/10.1109/DDCLS61622.2024.10606741>
10. Tang, S., Tian, D., Wu, X., Huang, M. & Deng, Y. Wind turbine load reduction based on 2DoF robust individual pitch control. *Renew. Energy*. <https://doi.org/10.1016/j.renene.2021.10.086> (2021).
11. Routray, A., Sivakumar, N., Huu S. & Bang, D. A. Comparative study of Optimal Individual Pitch Control methods. *Sustainability*. (2023). <https://doi.org/10.3390/su151410933>
12. Gaertner, E. et al. Definition of the IEA 15-Megawatt Offshore reference wind turbine (NREL/TP-75698). International Energy Agency. (2020). <https://www.nrel.gov/docs/fy20osti/75698.pdf>
13. Allen, C. et al. Definition of the UMaine VolturnUS-S reference platform developed for the IEA wind 15-Megawatt Offshore reference wind turbine (NREL/TP-76773). International Energy Agency. (2020). <https://www.nrel.gov/docs/fy20osti/76773.pdf>
14. Abbas, N. J., Wright, A. D. & Pao, L. Y. An Update to the National Renewable Energy Laboratory Baseline Wind Turbine Controller. *Journal of Physics: Conference Series*, 1452. (2020). <https://doi.org/10.1088/1742-6596/1452/1/012002>
15. An, Q. & Jiang, H. Research on coupled dynamic characteristics of Floating Wind Turbine under complex environment. *Journal of Physics: Conference Series*, 2473. (2023). <https://doi.org/10.1088/1742-6596/2473/1/012015>
16. Rony, J. S., Karmakar, D. & Soares, C. Coupled dynamic analysis of spar-type floating wind turbine under different wind and wave loading. *Mar. Syst. Ocean. Technol.* **16**, 169–198. <https://doi.org/10.1007/s40868-021-00106-7> (2021).
17. Johlas, H. M., Martínez-Tossas, L. A., Churchfield, M. J., Lackner, M. & Schmidt, D. P. Floating platform effects on power generation in spar and semisubmersible wind turbines. *Wind Energy*. <https://doi.org/10.1002/WE.2608> (2021).
18. Wen, B. et al. Wind shear effect induced by the platform pitch motion of a spar-type floating wind turbine. *Renew. Energy*. <https://doi.org/10.1016/j.RENENE.2018.12.034> (2019).
19. Dolan, D. & Lehn, P. W. Simulation model of wind turbine 3p torque oscillations due to wind shear and tower shadow. *IEEE Trans. Energy Convers.* **21**, 717–724. <https://doi.org/10.1109/PSCE.2006.296240> (2006).
20. Bin, Q. & Guo, B. Azimuth weight coefficient based independent variable pitch control strategy. *2013 Chin. Autom. Congress*, 143–147. <https://doi.org/10.1109/CAC.2013.6775717> (2013).
21. Morim, R. B., Carnielutti, F. D., Gründling, H. A. & Pinheiro, H. Robust model reference adaptive individual Pitch control for wind turbine load reduction. *IECON 2018–44th Annual Conf. IEEE Industrial Electron. Soc.* **1934–1939** <https://doi.org/10.1109/IECON.2018.8591621> (2018).
22. Tang, S., Tian, D., Fang, J., Liu, F. & Zhou, C. Individual pitch controller characteristics analysis and optimization under aerodynamic imbalanced loads of wind turbines. *Energy Rep.* <https://doi.org/10.1016/j.egyr.2021.09.114> (2021).
23. Lara, M., Garrido, J., van Wingerden, J., Mulders, S. P. & Vázquez, F. Optimization with genetic algorithms of individual pitch control design with and without azimuth offset for wind turbines in the full load region. *IFAC-PapersOnLine* <https://doi.org/10.1016/j.ifacol.2023.10.1591> (2023).

## Acknowledgements

The work was supported by the National Key R&D Program of China under grant number 2022YFB4201303.

## Author contributions

All authors contributed to the idea and control design of the study. D.X. Bai: Methodology, Software, Investigation, Writing. B. Wang: Methodology, Investigation, Writing. Y.S. Li: Methodology, Investigation, Software. W.C. Wang: Investigation, Resources, Funding Acquisition, Supervision.

## Declarations

### Competing interests

The authors declare no competing interests.

### Additional information

**Correspondence** and requests for materials should be addressed to B.W.

**Reprints and permissions information** is available at [www.nature.com/reprints](http://www.nature.com/reprints).

**Publisher's note** Springer Nature remains neutral with regard to jurisdictional claims in published maps and institutional affiliations.

**Open Access** This article is licensed under a Creative Commons Attribution-NonCommercial-NoDerivatives 4.0 International License, which permits any non-commercial use, sharing, distribution and reproduction in any medium or format, as long as you give appropriate credit to the original author(s) and the source, provide a link to the Creative Commons licence, and indicate if you modified the licensed material. You do not have permission under this licence to share adapted material derived from this article or parts of it. The images or other third party material in this article are included in the article's Creative Commons licence, unless indicated otherwise in a credit line to the material. If material is not included in the article's Creative Commons licence and your intended use is not permitted by statutory regulation or exceeds the permitted use, you will need to obtain permission directly from the copyright holder. To view a copy of this licence, visit <http://creativecommons.org/licenses/by-nc-nd/4.0/>.

© The Author(s) 2025